# Supplementary Material

**Supplementary Table 1**. Definitions of variants described in this work.

| Protein variant | Substitutions and modifications relative to parent |
|---|---|
| mTFP1[a] | = cFP484[b] + delete all residues before 6a and add MVSKGEE, H42N, L44I, S62T, N63T, Q66A, L72F, A80P, D81N, R123H, F124L, D125K, M127E, L141T, K142G, E144D, P145A, I149R, V158K, I161V, S162K, S164K, Y173H, C175V, S179T, K182R, V186A, L213V, N216S, Y221N, L223T, L224D, delete all residues after 224 and add GMDELYK. |
| mClavGR1[c] | = mTFP1 + G6dS, K17R, E34S, Y38F, D39E, N42Q, N45D, S57A, A66H, A71V, N81D, T96S, K102G, V105C, K106I, V107A, K108T, S109N, S112T, E115K, Y120N, E121K, L124F, D144E, R149K, H163M, E168K, H173Y, V175C, K178R, I180T, R182K, Q184a insertion, N203S, T212K, V213L, S216H, R220H, N221S, S222G, T223L, D224P |
| mClavGR1.1 | = mClavGR1 + T6bI, S34R, K36R, K74R, M113I, L166Q, Y173H |
| dClavGR1.6 | = mClavGR1 + T6bI, T41I, D77E, F99Y, K115E, E127V, K139R, A183V |
| mClavGR1.8 | = mClavGR1 + T6bI, T41I, D77E, F99Y, K115E, K139R, A183V |
| mClavGR2 | = mClavGR1 + T6bI, T41I, D77E, F99Y, K115E, E127T, K139R, A183V |

[a] Previously described.[1] [b] cFP484 is the wild-type protein from *Clavularia* (Genbank accession AAF03374).[2] [c] The key monomerizing mutations R123H, D125K, and M127E (of the A-B interface) and S162K and S164K (of the AC interface) of mTFP1 have been retained in mClavGR1.

**Supplementary Table 2.** Positions targeted for partial or complete randomization by mutagenesis. Figures were generated from PDB ID 2HQK[1] using MacPyMol (DeLano Scientific). Residues being substituted are indicated in red.

| Template | Residue(s) | Substitution(s) | Codon(s) | Result | Notes |
|---|---|---|---|---|---|
| mClavGR1 | I44 | All 20 amino acids | NNK | no improved variants | Close proximity to chromophore. Substitutions at residues 44 and 199 previously shown to benefit KikGR.[3] |
| | I199 | Leu, Ile, Met, Val, His, Gln, Asn, Lys Asp, Glu | VWK | | |
| mClavGR1 | T73 | All 20 amino acids | NNK | no improved variants | Previously reported to influence p$K_a$ of related FPs.[4] |
| dClavGR1.6 | F38 | All 20 amino acids | NNK | no improved variants | A cluster of residues located near the 'top' of the central helix. Substitution of residue 74 previously shown to benefit KikGR.[3] |
| | E39 | Asp, Glu, Gly, His, Lys, Asn, Gln, Arg, Ser | VRN | | |
| | K74 | Asp, Glu, Gly, His, Lys, Asn, Gln, Arg, Ser | VRN | | |
| mClavGR1.6 | E127V | Glu, Thr | GAA (Glu) ACB (Thr) | identified E127T | Disrupted residual dimerization tendency |
| dClavGR1.6 | K162 | All 20 amino acids | NNK | no improved variants | Adjacent to M163, which is in close proximity to the chromophore. K162A similar with K162K. |
| dClavGR1.6 | M163 | His or all 20 amino acids | CAY or NNK | no improved variants | Interacts with phenolate of chromophore. M163K brighter in green state but did not photoconvert to the red state. |
| mClavGR2 | F124 | Phe, Ile, Leu, Val | NTT | no improved variants | K125N similar to K125K |
| | K125 | His, Lys, Gln, Asn | AAM, MAG | | |
| | N128 | Pro, Arg, Ser, Thr | MSC | | |
| | F129 | Phe, Ile, Leu, Val | NTT | | |

**Supplementary Table 3**. Amino acid similarities (lower triangle) and identities (upper triangle) as calculated using MatGat[5] using the complete protein sequences provided in **Fig. 2**.

| | mTFP1 | mClavGR1 | mClavGR1.1 | mClavGR2 | mEos2 | Dendra2 | Kaede | mKikGR |
|---|---|---|---|---|---|---|---|---|
| **mTFP1** | | 81.9 | 80.2 | 79.3 | 62.4 | 66.9 | 59.1 | 59.3 |
| **mClavGR1** | 90.7 | | 97 | 96.6 | 77.6 | 70.2 | 75.1 | 71.5 |
| **mClavGR1.1** | 89.9 | 98.7 | | 94.5 | 75.5 | 68.5 | 73.8 | 70.2 |
| **mClavGR2** | 89 | 98.3 | 97.9 | | 76.4 | 69.3 | 73.8 | 71.1 |
| **mEos2** | 76.3 | 84.4 | 83.5 | 84.4 | | 70.9 | 83.2 | 71.7 |
| **Dendra2** | 78 | 81 | 81 | 80.6 | 84.1 | | 67.7 | 64.4 |
| **Kaede** | 76.3 | 84 | 84 | 83.5 | 91.6 | 82.7 | | 66.1 |
| **mKikGR** | 77.5 | 84.8 | 83.5 | 84.4 | 83.6 | 80.2 | 80.6 | |

**Supplementary Table 4**. Amino acid similarities (lower triangle) and identities (upper triangle) as calculated using MatGat[5] using only the sequence from position 6c to 224 in **Fig. 2**.

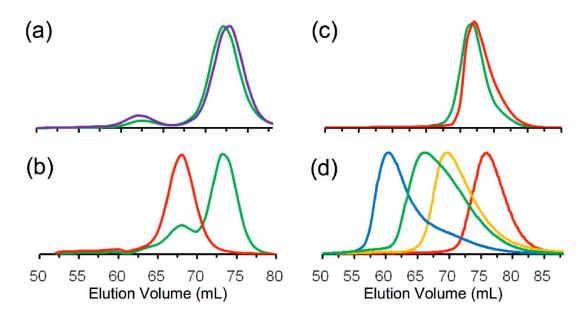|  | mTFP1 | mClavGR1 | mClavGR1.1 | mClavGR2 | mEos2 | Dendra2 | Kaede | mKikGR |
|---|---|---|---|---|---|---|---|---|
| **mTFP1** |  | 80.5 | 79.2 | 78.3 | 66.5 | 71.8 | 62.4 | 63.2 |
| **mClavGR1** | 90 |  | 97.3 | 96.8 | 82.8 | 74.2 | 79.6 | 76.3 |
| **mClavGR1.1** | 89.6 | 99.1 |  | 94.1 | 80.5 | 72.4 | 78.3 | 75 |
| **mClavGR2** | 88.7 | 98.6 | 97.7 |  | 81.4 | 73.3 | 78.3 | 75.9 |
| **mEos2** | 80.5 | 89.6 | 88.7 | 89.6 |  | 71 | 84.2 | 74.1 |
| **Dendra2** | 83.2 | 85.1 | 85.1 | 84.6 | 83.7 |  | 67.9 | 65.9 |
| **Kaede** | 79.6 | 88.7 | 88.7 | 88.2 | 92.3 | 82.4 |  | 68.3 |
| **mKikGR** | 80.7 | 88.8 | 87.4 | 88.3 | 86.1 | 82.1 | 83.4 |  |

**Supplementary Table 5**. Amino acid differences between green-to-red proteins, considering only those residues with side chains directed towards the interior of the β-barrel. Amino acids that differ from mClavGR2 are shaded gray.

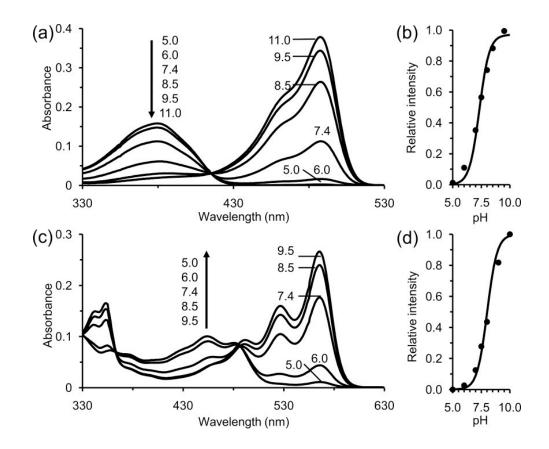| Position | mClavGR2 | mEos2 | Dendra2 | Kaede | mKikGR |
|---|---|---|---|---|---|
| 14 | I | I | V | I | I |
| 16 | L | L | V | L | L |
| 44 | I | M | A | M | V |
| 52 | A | G | A | A | G |
| 57 | A | A | S | A | A |
| 58 | Y | F | Y | Y | F |
| 65 | F | F | V | F | F |
| 73 | T | A | T | A | V |
| 91 | Y | Y | Y | F | Y |
| 97 | M | L | M | L | M |
| 99 | Y | F | F | F | Y |
| 107 | A | A | I | A | A |
| 109 | N | N | S | N | N |
| 120 | N | N | Q | N | N |
| 122 | I | V | V | V | I |
| 150 | M | M | L | M | M |
| 161 | V | I | I | I | V |
| 183 | V | A | A | S | A |
| 199 | I | I | I | I | M |
| 213 | L | L | L | L | A |
| **# differences from mClavGR2** | | 9 | 13 | 8 | 7 |

**Supplementary Table 6**. Sum of the number of differences between green-to-red proteins, considering only those residues with side chains directed towards the interior of the β-barrel.
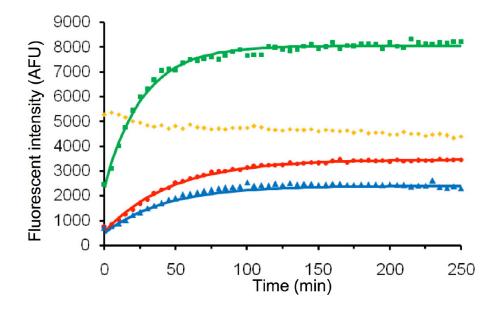
|  | mEos2 | Dendra2 | Kaede | mKikGR |
|---|---|---|---|---|
| **mClavGR2** | 9 | 13 | 8 | 7 |
| **mEos2** |  | 13 | 4 | 8 |
| **Dendra2** |  |  | 13 | 17 |
| **Kaede** |  |  |  | 12 |

**Supplementary Fig. 1.** Characterization of the oligomeric structure of mClavGR2, mEos2, and Dendra2 by gel filtration chromatography. (a) Coinjection of mCherry and mClavGR2 with detection at both 488 nm (green) and 585 nm (violet). The identity of the species eluting at approximately 63 min is currently unknown, but it was not observed when the sample was first purified with gel filtration as in panel (c). (b) Coinjection of mClavGR2 and dTomato with detection at both 488 nm (green) and 555 nm (red). (c) Overlaid elution profiles from separate injections of 1 mM mClavGR2 (green) and 1 mM Dendra2 (red) with detection at 488 nm. (d) Overlaid elution profiles from separate injections of mEos2 at variant concentrations with detection at 488 nm. The concentrations of the samples are 1 mM (blue), 0.5 mM (green), 0.1 mM (yellow) and 0.01 mM (red).
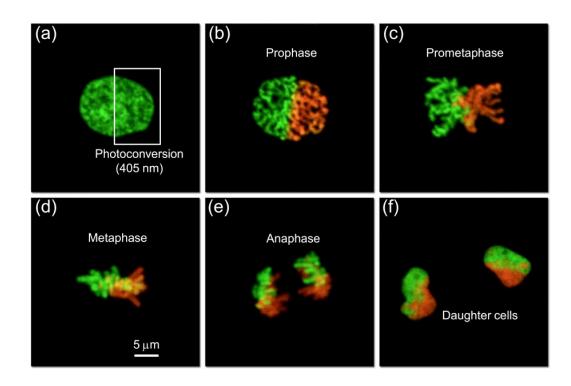
**Supplementary Fig. 2**. Characterization of the pH dependence of the green and red states of mClavGR2. (a) Absorbance spectra of the pre-photoconversion green state of mClavGR2 at pH values ranging from 5 to 11. (b) Plot of relative intensity at 490 nm as a function of pH. The line represents the best fit of the data using the Henderson-Hasselbalch equation and is consistent with a p$K_a$ of 8.0. (c) Absorbance spectra of the post-photoconversion red state of mClavGR2 at pH values ranging from 5 to 11. (d) Plot of relative intensity at 570 nm as a function of pH and it as in panel (b). The fit is consistent with a p$K_a$ of 7.3.
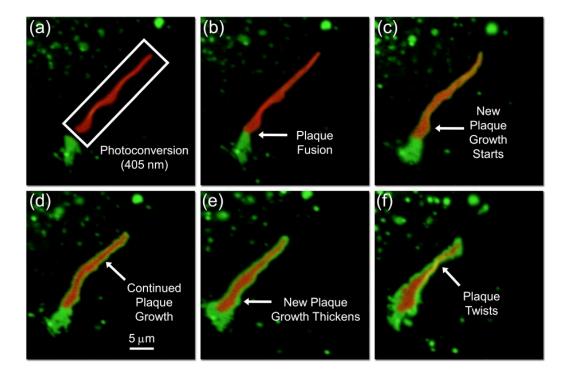
**Supplementary Fig. 3**. Maturation of monomeric photoconvertible FPs at 37°C. The maturation profiles of mClavGR2 (green), mClavGR1 (red), and Dendra2 (blue) can be fit as monoexponential curves with time constants of 27 min, 47 min and 42 min, respectively. Under the conditions of this experiment, mEos2 (yellow) appears to have fully matured prior to the initial measurement. Each curve represents the average of two independent experiments.
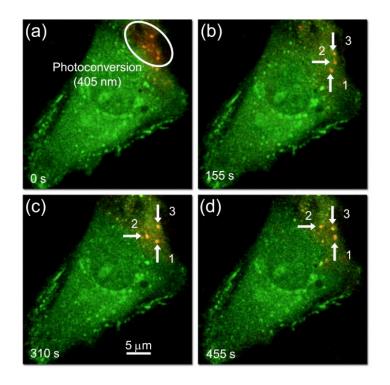
**Supplementary Fig. 4**. Photobleaching curves for mClavGR variants. All curves have been normalized to an initial fluorescence emission rate of 1,000 photons/molecule/second. (a) Widefield photobleaching of the green state. (b) Confocal photobleaching of the green state. (c) Widefield photobleaching of the red state. (d) Confocal photobleaching of the red state.

**Supplementary Fig. 5**. Photoconversion and imaging of H2B-mClavGR2. These frames are taken from **Supplementary Movie 1**. (a) The photoconverted region is indicated with a white rectangle. (b-e) Progression through mitosis. (f) Daughter cells.

**Supplementary Fig. 6**. Photoconversion and imaging of Cx43-mClavGR2. These frames are taken from **Supplementary Movie 2**. (a) The photoconverted region is indicated with a white rectangle. (b-f) Time lapse images of a plaque fusion event and new plaque growth from the edges of the gap junction.

**Supplementary Fig. 7**. Photoconversion and imaging of endosomes with Rab5a-mClavGR2. These frames are taken from **Supplementary Movie 3**. (a) The photoconverted region is indicated with a white oval. (b-d) Time lapse tracking of the dynamic localization of 3 individual endosomes.

# Supplementary References

1. Ai H., Henderson J. N., Remington S. J. & Campbell R. E. (2006). Directed evolution of a monomeric, bright and photostable version of Clavularia cyan fluorescent protein: structural characterization and applications in fluorescence imaging. *Biochem. J.* **400**, 531-540.

2. Matz M. V., Fradkov A. F., Labas Y. A., Savitsky A. P., Zaraisky A. G., Markelov M. L. & Lukyanov S. A. (1999). Fluorescent proteins from nonbioluminescent Anthozoa species. *Nat. Biotechnol.* **17**, 969-973.

3. Tsutsui H., Karasawa S., Shimizu H., Nukina N. & Miyawaki A. (2005). Semi-rational engineering of a coral fluorescent protein into an efficient highlighter. *EMBO Rep.* **6**, 233-238.

4. Adam V., Nienhaus K., Bourgeois D. & Nienhaus G. U. (2009). Structural basis of enhanced photoconversion yield in green fluorescent protein-like protein Dendra2. *Biochemistry* **48**, 4905-4915.

5. Campanella J. J., Bitincka L. & Smalley J. (2003). MatGAT: an application that generates similarity/ identity matrices using protein or DNA sequences. *BMC Bioinformatics* **4**, 29.